



## Classical Dynamical Localization

Italo Guarneri,<sup>1,2</sup> Giulio Casati,<sup>1,3,4</sup> and Volker Karle<sup>5</sup>

<sup>1</sup>*Center for Nonlinear and Complex Systems, Università degli Studi dell'Insubria, Via Valleggio 11, 22100 Como, Italy*

<sup>2</sup>*Istituto Nazionale di Fisica Nucleare, Sezione di Pavia, Via Bassi 6, 27100 Pavia, Italy*

<sup>3</sup>*International Institute of Physics, Federal University of Rio Grande do Norte, 59708-400 Natal-RN, Brazil*

<sup>4</sup>*CNISM and Istituto Nazionale di Fisica Nucleare, Sezione di Milano, Via Celoria 16, 20133 Milano, Italy*

<sup>5</sup>*Albert-Ludwigs Universität Freiburg, D-79104 Freiburg im Breisgau, Germany*

(Received 6 August 2014; published 20 October 2014)

We consider classical models of the kicked rotor type, with piecewise linear kicking potentials designed so that momentum changes only by multiples of a given constant. Their dynamics display quasilocalization of momentum, or quadratic growth of energy, depending on the arithmetic nature of the constant. Such purely classical features mimic paradigmatic features of the quantum kicked rotor, notably dynamical localization in momentum, or quantum resonances. We present a heuristic explanation, based on a classical phase space generalization of a well-known argument, that maps the quantum kicked rotor on a tight-binding model with disorder. Such results suggest reconsideration of generally accepted views that dynamical localization and quantum resonances are a pure result of quantum coherence.

DOI: [10.1103/PhysRevLett.113.174101](https://doi.org/10.1103/PhysRevLett.113.174101)

PACS numbers: 05.45.Mt, 72.15.Rn

Dynamical localization in the quantum kicked rotor (QKR) is a prototypical example of how quantization can drastically modify the qualitative features of classical chaotic motion [1–3]. It is assimilated to the Anderson localization in disordered solids [3,4], and, like the latter, it is considered to be an effect of quantum interference. Dynamical localization is also expected with kicked particles moving in a line. Experimental observations on kicked cold atoms [5] support such expectations, which are all the more natural, because quantum kicked rotors and quantum kicked particles are closely connected by Bloch theory [6]: spatial periodicity enforces conservation of quasimomentum, and the dynamics at fixed quasimomentum are those of a generalized QKR [7]. Thus a crucial difference between the quantum and the classical dynamics of kicked particles is immediately apparent: notably, the former have a constant of the motion, while the latter have none. In this Letter, we submit that exactly this difference plays a major role in the dynamical localization effect. We base our results on a family of classical dynamical systems, which are subject to a purely classical conservation law for quasimomentum. These are models of the kicked rotor (KR) type, where the kicking potentials are a piecewise, continuous,  $2\pi$ -periodic, function so that kicks can change momentum only by integer multiples of a constant  $\eta > 0$ . They will be termed generalized triangle maps (GTM) because they include as a particular example the triangle map [8,9], that despite its formal simplicity still challenges exact analysis.

In this connection, we'd like to recall a seminal paper [10] in which the question was raised, whether the quantum inhibition of classical chaotic effects could be somehow explained by a “discreteness of quantum phase space.”

Following this idea, the classical kicked rotor was artificially discretized, and a limitation of the chaotic diffusion was observed. Classical maps of the same kind have later been derived in a different way in Ref. [11], and named “classical models of quantum stochasticity.” These *ad hoc* discretized models have been confirmed to reproduce some quantum effects, like resonances, and limitations of chaotic diffusion.

Here we provide empirical and analytical evidence that purely classical models described by GTMs, indeed offer an intriguing imitation of the QKR. Our numerical results show that for strongly irrational  $\eta/(2\pi)$ , the KR diffusion is replaced by localization, or by “quasilocalization,” i.e., very slow (power-logarithmic) transport in momentum space. If averaged over quasimomenta, the quasilocalized momentum distributions display a clean exponential shape. For rational  $\eta/(2\pi)$ , and quasimomentum commensurate to  $2\pi$ , quadratic growth of energy is observed, similar to the QKR resonances [7].

Quasilocalization, instead of strict localization as in QKR, is likely to be due to the absence of interference in GTMs. Each kick changes the QKR state to a new state, where jumps by different multiples of  $\hbar$  are coherently superposed and interfere in ways that have no counterpart in GTMs. Thus, in spite of general parallelism, differences still exist between the GTM and the QKR dynamics, that reflect the fundamental difference of classical and quantum mechanics. That such differences leave room for classical lookalikes of dynamical localization and resonances suggests the reassessment of commonplace views, that the latter effects are pure manifestations of quantum coherence.

Proper explanation of such numerical results demands a purely classical analysis of the GTMs. An exact argument to be reviewed later shows that GTM resonances have

exactly the same origin as the QKR resonances, notably, conservation of quasimomentum, together with translation invariance (in momentum space). For quasilocization, we instead present a heuristic argument that, somewhat paradoxically, is of a quantum origin. It is based on a construction due to Fishman, Grepel, and Prange (FGP) [3,4,12] that maps the QKR on a 1D tight-binding model with pseudorandom disorder. We first reformulate that mapping in the Weyl phase space representation of quantum mechanics. The QKR is thereby turned into a 2D tight-binding model with short-range hopping amplitudes and on-site potentials that are periodic at resonances and pseudorandom for sufficient incommensuration; in the latter case, exponential localization is inferred. The two directions in the lattice respectively correspond to momentum and to the harmonics of position. Next we note that, thanks to the special features of GTMs, the very same construction can be used to map the unitary Perron-Frobenius (PF) operator of GTMs on a 2D lattice model. Pseudorandomness is the same as for the QKR and couplings are still short range in the direction of momentum; however, in the other direction they are now long range. The same line of reasoning that so successfully works in the QKR case, now leads us to predict localization in momentum, and delocalization in the harmonics of position.

The GTMs we consider in this Letter are strictly classical maps of the form

$$p_{t+1} = p_t + V'(\theta_t), \quad \theta_{t+1} = \theta_t + p_{t+1}, \quad (1)$$

where  $V(\theta)$  is a continuous,  $2\pi$ -periodic, piecewise linear potential, such that the possible values of  $V'(\theta)$  (“channels”) are a finite set of multiples of a constant  $\eta > 0$ , and  $V(\theta + \pi) = -V(\theta)$ . In this Letter we choose  $V(\theta)$  as illustrated in Fig. (1). The map may also be read as a dynamical system in the 2-torus. Except for the fact that they are not chaotic, very little is known about such toral maps, even in the case when  $V'(\theta)$  only takes two values

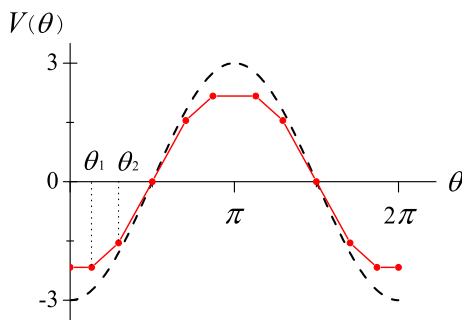


FIG. 1 (color online). The periodic potential  $V(\theta)$  (red solid line) is linear in between any two subsequent points  $\theta_n$  where  $\mu \sin(\theta_n)/\eta$  takes integer values (only those in  $[0, \pi/2]$  are shown). Its piecewise constant slope is  $V'(\theta) = j(\theta)\eta$  where  $j(\theta)$  is the integer that rounds  $\mu \sin(\theta)/\eta$  toward 0; here  $\mu = 3, \eta = 1.2$ . In the limit of vanishing  $\eta$ ,  $V(\theta)$  converges to the standard kicked rotor potential (dashed curve).

[9,13]. In that case, the map is similar to a “triangle map” that describes the motion of a point mass in a right-triangular billiard. Ergodicity of such billiards is a long-standing issue, and in a recent paper [14] contrary indications in that respect have been surmised, based on the observation of a phenomenon there dubbed “exponential localization of invariant measures.” It is easily proven that the strict localization of the map in Eq. (1) would forbid ergodicity of the corresponding toral map. A typical phase portrait of a toral map [Eq. (1)] is shown in the Supplemental Material [15].

At all times  $t$ ,  $p_t = \beta + n_t\eta$ , with  $n_t$  integer and where the quantity  $\beta \equiv \text{mod}(p, \eta)$  is invariant under the map. The dynamics are thus described by the map

$$n_{t+1} = n_t + V'(\theta_t)/\eta, \quad \theta_{t+1} = \theta_t + \beta + n_{t+1}\eta. \quad (2)$$

In our numerical investigation we have used GTMs with 3,5,7 channels. Results are shown in Figs. 2 and 3 and

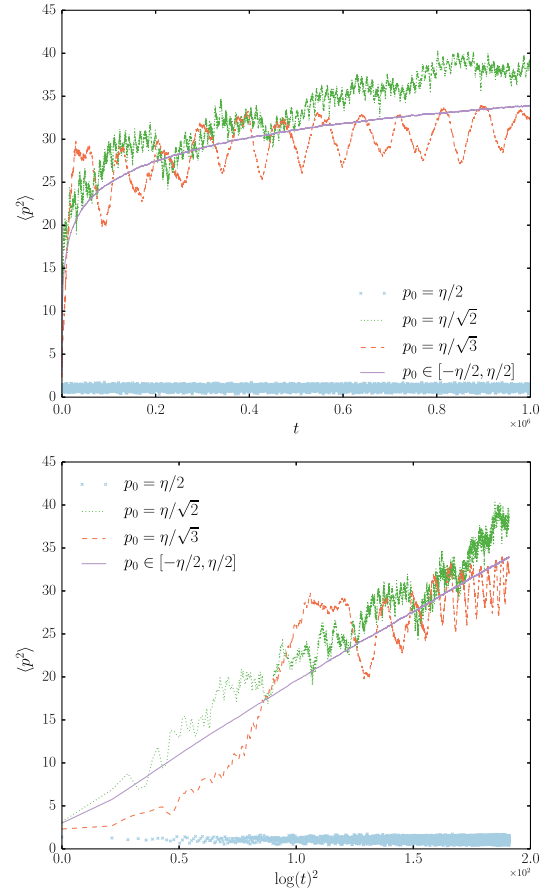


FIG. 2 (color online).  $\langle p^2 \rangle$  of GTMs averaged over an ensemble of  $10^6$  initial points with  $\theta_0$  randomly distributed in  $(0, 2\pi)$ , versus time  $t$  (upper plot) and versus  $\log(t)^2$  (lower plot). Here  $\eta = \pi/\text{GM}$  (where GM is the golden mean),  $\mu = 3$ , and  $p_0 = \eta/2, \eta/\sqrt{2}, \eta/\sqrt{3}$ . Blue lines represent averages over  $5 \times 10^6$  initial points ( $\theta_0, p_0$ ) randomly distributed in  $(0, 2\pi) \times (-\eta/2, \eta/2)$ . All curves were averaged over 100 iterations.

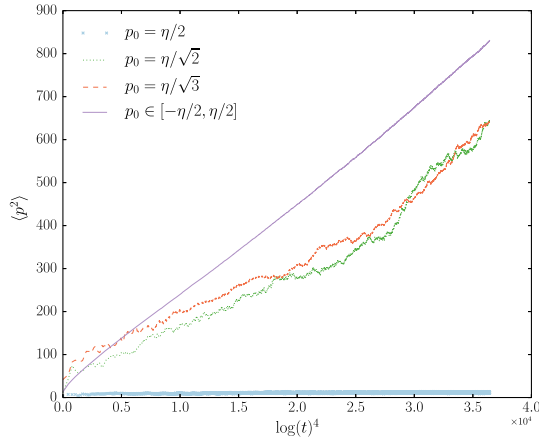


FIG. 3 (color online). Same as Fig. 2 (lower) but with  $\mu = 4$

crucially depend on the arithmetics of the triple  $\eta, \beta, \pi$ . With  $\eta$  strongly incommensurate to  $\pi$ , and  $\beta$  a low-order rational multiple of  $\eta$ , the average energy of ensembles with randomly generated  $\theta_0$  undergoes strict localization (lowest curves). For  $\beta$  incommensurate to  $\eta$ , we observe quasilocization, i.e., slow, somewhat erratic growth of energy not faster than power logarithmic, with an exponent that appears to depend on the number of channels. Additionally averaging over quasimomentum yields clean indications in this sense (solid lines). The  $\beta$ -averaged, quasilocalized momentum distributions show a remarkably clean exponential decay away from a central tiny peak (Fig. 4). The time scale for the onset of such exponential distributions rapidly increases on decreasing  $\eta$ , as the initial spreading in momentum approaches the classical diffusion of the kicked rotor. At small  $\eta$  numerical analysis of the quasilocalized regime becomes a prohibitive computational task. When  $\beta, \eta$ , and  $\pi$  are mutually commensurate, ballistic momentum growth is observed, at least for sufficiently

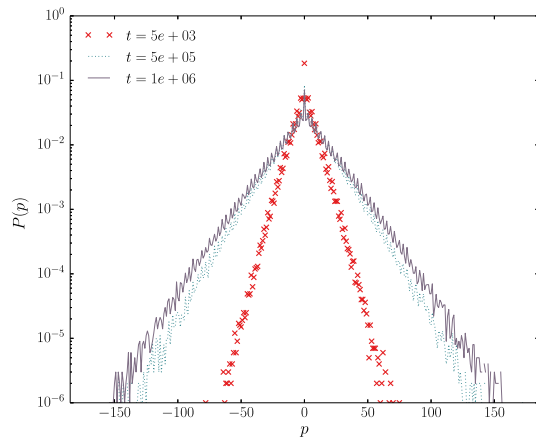


FIG. 4 (color online). Momentum distributions for ensembles of  $5 \times 10^6$  initial points  $(\theta_0, p_0)$  randomly distributed in  $(0, 2\pi) \times (-\eta/2, \eta/2)$ ,  $\mu = 4$ , and  $\eta/\pi = \text{GM}$ . The curves are averaged over the last 100 kicks.

large values of  $\mu/\eta$ . If  $\eta$  is identified with an effective Planck constant, this behavior reproduces the quantum resonances of the generalized QKR [7] (except for the fact that the latter do not depend on the kicking strength). This is explained as follows [11]. Let  $\beta$  and  $\eta$  be commensurate:  $\beta s = \eta r \equiv rs\lambda$ , with  $r, s$  coprime integers. Then, at all times  $t$ ,  $p_t = N_t\lambda$  and  $\theta_t = \theta_0 + M_t\lambda$  with  $N_t, M_t$  integers. Then Eq. (2) yields the following map for the integers  $N_t$  and  $M_t$ ,

$$N_{t+1} = N_t + \Phi(M_t), \quad M_{t+1} = M_t + N_{t+1}, \quad (3)$$

where, for fixed  $\theta_0$ ,  $\Phi(M_t) \equiv \lambda^{-1}V'(\theta_0 + M_t\lambda)$  is an integer valued quasiperiodic function, with a finite number of values. If in addition  $\eta$  (and hence  $\lambda$ ) is commensurate to  $2\pi$ ,  $\lambda = 2\pi p/q$  with  $p, q$  coprime integers, then  $\Phi$  is periodic, and the map in Eq. (3) commutes with translations of both variables by multiples of  $q$ . Therefore, it defines a map  $\mathcal{M}$  of the discrete 2-torus  $\mathbb{T}_q \times \mathbb{T}_q$  in itself, where  $\mathbb{T}_q$  is the set of congruence classes mod  $(q)$ . As  $\mathcal{M}$  is bijective in a finite set, all its trajectories are periodic; so, for all choices of  $\theta_0$  and  $p_0$  which are consistent with the given  $\beta$ , there are a period  $T$  and integers  $K, L$  so that  $\theta_{mT} = \theta_0 + Km q \lambda \text{ mod } (2\pi)$  and  $p_{mT} = p_0 + Lm q \lambda$  for all integers  $m$ . If the number of channels is sufficiently large, some orbits have  $L > 0$ ; along such orbits the momentum  $p_t$  increases, on the average, proportional to  $Lq\lambda t/T$ . Quadratic growth of the mean energy follows.

Next we show that a theoretical understanding about the purely classical GTM can be obtained from quantum localization theory. To this end we consider the PF operator  $\hat{U}_{\text{GTM}}$  for the GTM dynamics. For given  $\beta$ , the phase space of the map in Eq. (2) is  $\Omega = \mathbb{T} \times \mathbb{Z}$  and  $\hat{U}_{\text{GTM}}$  unitarily acts on square-summable functions  $\Psi \in L^2(\Omega)$  so that  $\hat{U}_{\text{GTM}}\Psi(\theta_t, n_t) = \Psi(\theta_{t-1}, n_{t-1})$ . To the unitary operator  $\hat{U}_{\text{GTM}}$  we will associate a 2D lattice problem, implementing the FGP construction that was used [4] to map the quantum kicked rotor on a 1D lattice problem. Here we outline this calculation, leaving details for the Supplemental Material [15]. We first derive a phase-space version of the FGP construction and to this end we exploit the Weyl correspondence  $\mathfrak{B}$ , that maps Hilbert-Schmidt operators  $\hat{A}$  (e.g., states) in the Hilbert space of the QKR to the square-summable function  $\Psi = \mathfrak{B}(\hat{A})$  on  $\Omega$ , according to

$$\Psi(\theta, n) = \frac{1}{\sqrt{2\pi}} \sum_{l \in \mathbb{Z}} \langle e_l | \hat{A} | e_{n-l} \rangle e_{2l-n}(\theta) \quad (4)$$

$$= \int_0^{2\pi} d\theta' \langle \theta' | \hat{A} | 2\theta - \theta' \rangle e_n(\theta - \theta'), \quad (5)$$

where  $e_l(\theta) = (2\pi)^{-1/2} \exp(il\theta)$ . As  $\hat{A}$  evolves into  $\hat{U} \hat{A} \hat{U}^\dagger$  where  $\hat{U}$  is some unitary evolution operator, its Weyl representative  $\Psi$  evolves into  $\hat{U}\Psi = \mathfrak{B}(\hat{U}\mathfrak{B}^{-1}(\Psi)\hat{U}^\dagger)$ . This defines the unitary propagator  $\hat{U}$  in  $L^2(\Omega)$  that

describes evolution in the Weyl representation. Let, in particular,  $\hat{U}$  be the Floquet operator  $\hat{U}_{\text{KR}}$  of the QKR with quasimomentum  $\beta$ :  $\hat{U}_{\text{KR}} = \exp(-i\hat{V}_{\text{KR}}) \exp(-i\hat{T})$ , where

$$V_{\text{KR}} = \hbar^{-1}\mu \cos(\theta), \quad \hat{T} = \hbar^{-1}(-i\hbar \frac{d}{d\theta} + \beta)^2/2. \quad (6)$$

After a calculation based on Eqs. (4) and (5), we find that

$$\hat{U}_{\text{KR}} = \exp(-i\hat{V}_{\text{KR}}) \exp(-i\hat{T}), \quad (7)$$

where

$$\hat{T} = -i\left(\frac{1}{2}\hbar n + \beta\right) \frac{d}{d\theta}, \quad (8)$$

$$\mathfrak{F}\hat{V}_{\text{KR}}\Psi(\theta, \varphi) = -2\mu\hbar^{-1} \sin(\theta) \sin(\varphi)\mathfrak{F}\Psi(\theta, \varphi), \quad (9)$$

where  $\mathfrak{F}$  denotes the Fourier transform:  $\mathfrak{F}\Psi(\theta, \varphi) \equiv \sum_n \Psi(\theta, n) e_n(\varphi)$ . At this point we come to the FGP construction. In its original version [3,4], it maps the QKR eigenvalue equation  $\hat{U}_{\text{KR}}\psi = e^{i\omega}\psi$  on a 1D tight-binding problem. The equation is indeed equivalent to  $(\hat{W} + \hat{Z})\phi = 0$ , where  $\hat{W}$  and  $\hat{Z}$  are inverse Cayley transforms of  $\exp(-i\hat{V}_{\text{KR}})$  and  $\exp[-i(\hat{T} + \omega)]$ , respectively, and  $\phi = (i + \hat{Z})^{-1}\psi$ . Now  $\exp[-i(\hat{T} + \omega)]$  (hence  $\hat{Z}$ ) has a pure point spectrum,  $\exp(-i\hat{V}_{\text{KR}})$  (hence  $\hat{W}$ ) is invariant under translations over the eigenbasis of  $\hat{T}$ , and if  $\mu < \pi$  then  $W$  is bounded so, written in that basis,  $(\hat{W} + \hat{Z})$  looks like a lattice Hamiltonian, where the eigenvalues of  $\hat{Z}$  play the role of on-site potentials, and  $\hat{W}$  describes hopping between sites. This construction works unaltered if  $\hat{U}_{\text{KR}}$  is replaced by any operator (in an arbitrary Hilbert space) that comes in the form of a product of two unitary operators with the above properties. For  $\mu < \pi/2$  this is the case with  $\hat{U}_{\text{KR}}$  thanks to Eqs. (7), (8), and (9), and FGP immediately yields the following 2D lattice equation:

$$\sum_{n', k' \in \mathbb{Z}} W_{n-n', k-k'} \Phi_{n'k'} + Z_{nk}(\omega) \Phi_{nk} = 0, \quad (10)$$

where  $Z_{nk}(\omega) \equiv \tan[\chi_{nk}(\omega)]$ ,  $\chi_{nk}(\omega) = [\omega - (n\hbar/2 + \beta)k]/2$ . For  $\mu < \pi\hbar/2$  the couplings  $W_{n,k}$  are the Fourier coefficients of the analytic function  $\tan[\mu\hbar^{-1} \sin(\theta) \sin(\varphi)]$  so they decay exponentially fast, and Eq. (10) is formally similar to an eigenvalue equation for a 2D tight-binding model with short-range hopping. When  $\hbar$  is strongly incommensurate to  $2\pi$ , the potential is pseudorandom, and exponential localization follows. At resonances  $\hbar$  and  $\beta$  are commensurate to  $2\pi$ , so the potential is periodic, enforcing extended eigenfunctions, and ballistic propagation.

This construction is not applicable as it is when  $\mu > \pi\hbar/2$ , because then  $\tan[\mu\hbar^{-1} \sin(\theta) \sin(\varphi)]$  has non-integrable singularities. This difficulty is circumvented by an improved method [12]. For the Weyl representation of the QKR, this method replaces Eq. (10) by

$$\sum_{n', k'} |\tilde{W}_{n-n', k-k'}| \sin(\chi_{n'k'}(\omega) + \phi_{n-n', k-k'}) \tilde{\Phi}_{n'k'} = 0, \quad (11)$$

where  $\tilde{W}_{n,k}$  are the Fourier coefficients of  $e^{-i\nu_{\text{KR}}(\theta, \varphi)/2}$ , and  $\phi_{n,k}$  are their phases [16]. In this formulation, disorder also appears in couplings, which still decay exponentially fast.

We've thus rephrased the FGP construction for the QKR in the phase-space representation. This was possible, thanks to a special structure of the Weyl propagator of the QKR, as a unitary operator in  $L^2(\Omega)$ . Now we'll show that the same is true with the completely classical PF operator of GTMs. To see this, just replace  $\hbar$  by  $\eta$  throughout, and let the prefactor of  $\mathfrak{F}\Psi$  on the right-hand side of Eq. (9) be replaced by  $2\varphi V'(\theta)/\eta$ . Then, instead of  $\hat{V}_{\text{KR}}$ , Eq. (9) defines a new operator  $\hat{V}_{\text{GTM}}$ , and it is easily seen that

$$e^{-i\hat{V}_{\text{GTM}}}\Psi(\theta, n) = \Psi[\theta, n - 2V'(\theta)/\eta]. \quad (12)$$

Using Eqs. (7) and (8), the full propagator  $\hat{U}_{\text{KR}}$  is replaced by

$$\hat{U}_{\text{GTM}}\Psi(\theta, n) = \Psi(\theta', n'), \quad (13)$$

$$\theta' = \theta - \eta n/2 - \beta, \quad n' = n - 2V'(\theta')/\eta.$$

Restricting to even values  $n$ , and rescaling  $n$  by  $1/2$ , the map in Eq. (13) is the inverse of the reduced GTM map [Eq. (2)], so  $\hat{U}_{\text{GTM}}$  is the PF operator for the dynamical system [Eq. (2)]. This opens the way to mapping on a 2D lattice model.  $\hat{V}_{\text{KR}}$  has to be replaced by  $\hat{V}_{\text{GTM}}$ , so the improved formulation [Eq. (11)] is necessary, because  $\tan(\varphi V'(\theta)/\eta)$  has nonintegrable singularities. "Disorder" is the same, but couplings are different:

$$\tilde{W}_{n-n', k-k'} = \frac{1}{2\pi} \int_{I_{n-n'}} d\theta e^{-i(k-k')\theta},$$

where  $I_n$  is the interval wherein  $2V'(\theta) = n\eta$ . In the  $n$  direction (momentum) such couplings vanish whenever  $|n - n'|\eta$  is larger than the maximum of  $|V'(\theta)|$ . In the  $k$  direction (harmonics of position) they slowly decay proportional to  $|k - k'|^{-1}$  due to discontinuities of  $V'(\theta)$ . On such grounds, whenever  $\eta$  is incommensurate to  $\pi$  we are led to expect (i) localization in momentum, and (ii) delocalization over the harmonics of position. We consider (i) to be consistent with numerical results, because the argument is too crude to discriminate quasilocalization from strict localization; inferring the power-logarithmic spreading from the 2D lattice dynamics is a nontrivial interesting problem. At variance with QKR, (ii) implies a continuous GTM spectrum in all cases. In order to check (ii), we have numerically computed the PF evolution of a given function of  $n$  and  $\theta$ . Fourier expansion at each time  $t$  yields amplitudes  $f_{nk}(t)$  at the sites in the 2D lattice. Our numerical results show that the distribution

$P(k, t) \equiv \sum_n |f_{nk}(t)|^2$  rapidly spreads over the whole available Fourier basis.

Our present evidence of GTM quasilocalization and resonances is for cases when  $\eta/\pi$  is either strongly irrational (in fact, equivalent to the golden mean), or rational. A better understanding of this intriguing dynamical behavior will require analysis of how it depends on the degree of irrationality of  $\eta/\pi$ .

Useful discussions with Shmuel Fishman are gratefully acknowledged. This work is supported by MIUR-PRIN.

- 
- [1] G. Casati, B. V. Chirikov, F. M. Izrailev, and J. Ford, in *Stochastic Behavior in Classical and Quantum Hamiltonian Systems*, Lecture Notes in Physics Vol. 93 (Springer, Berlin, 1979), p. 334.
- [2] F. M. Izrailev, *Phys. Rep.* **196**, 299 (1990).
- [3] S. Fishman, in *Proceedings of the International School of Physics “Enrico Fermi,” Course CXIX*, edited by G. Casati, I. Guarneri, and U. Smilansky (North-Holland, Amsterdam, 1993), p. 187, and references therein.
- [4] S. Fishman, D. R. Grempel, and R. E. Prange, *Phys. Rev. Lett.* **49**, 509 (1982).
- [5] M. Raizen and D. L. Steck, *Scholarpedia* **6**, 10468 (2011).
- [6] S. Fishman, I. Guarneri, and L. Rebuzzini, *J. Stat. Phys.* **110**, 911 (2003).
- [7] I. Dana and D. L. Dorofeev, *Phys. Rev. E* **73**, 026206 (2006).
- [8] G. Casati and T. Prosen, *Phys. Rev. Lett.* **85** (2000) 4261.
- [9] M. Horvat, M. Degli Esposti, S. Isola, T. Prosen, and L. Bunimovich, *Physica (Amsterdam)* **238D**, 395 (2009).
- [10] B. V. Chirikov, F. M. Izrailev, and D. L. Shepelyansky, *Sov. Sci. Rev. Sect. C* **2**, 209 (1981).
- [11] G. P. Berman, A. R. Kolovsky, and F. M. Izrailev, *Physica (Amsterdam)* **152A**, 273 (1988); G. P. Berman, A. R. Kolovsky, F. M. Izrailev, and A. M. Iomin, *Chaos* **1**, 220 (1991).
- [12] D. L. Shepelyansky, *Phys. Rev. Lett.* **56**, 677 (1986).
- [13] This is, e.g., the case of the “sawtooth map”: L. Kaplan and E. Heller, *Physica (Amsterdam)* **121D**, 1 (1998).
- [14] J. Wang, G. Casati, and T. Prosen, *Phys. Rev. E* **89**, 042918 (2014).
- [15] See Supplemental Material at <http://link.aps.org/supplemental/10.1103/PhysRevLett.113.174101> for details.
- [16] The self-adjoint Hamiltonian underlying Eq. (11) is (in operator form) [12]  $\hat{H} = \cos(\frac{1}{2}\hat{V}_{\text{KR}}) \tan(\frac{1}{2}\omega - \frac{1}{2}\hat{T}) \times \cos(\frac{1}{2}\hat{V}_{\text{KR}}) - \frac{1}{2}\sin(\hat{V}_{\text{KR}})$ .